CHAPTER 4

MECHANISM OF FILM FORMATION

4.1 Formation Stages of Thin Films

It has been found by observation of films evaporated directly in the viewing field of an electron microscope that film growth may be divided into certain stages. These are as follows:

(1) Nucleation, during which small nuclei are formed that are statistically distributed (with some exceptions) over the substrate surface.

(2) Growth of the nuclei and formation of larger islands, which often have the shape of small crystals (crystallites).

(3) Coalescence of the islands (crystallites) and formation of a more or less connected network containing empty channels.

(4) Filling of the channels.

The process is schematically shown in Fig. 39. (It should be noted that Fig. 39a shows nuclei already formed because at the birth stage the
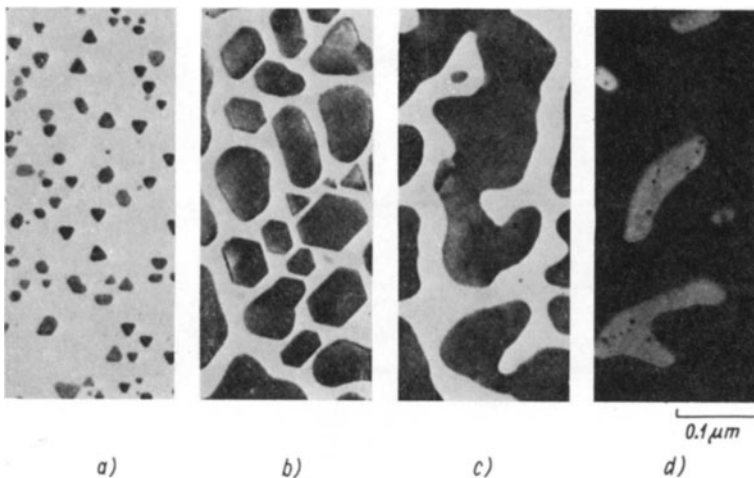

0.1 μm

a)   b)   c)   d)

Fig. 39: Process of formation of Ag film on MoS$_2$ (Pashley [26]).

nuclei dimensions are usually beyond the resolving power of an electron microscope.)

It is important to note that after a certain concentration of nuclei is reached additional impinging particles do not form further nuclei but adhere to the existing ones or to the islands formed already. As we shall see later, the nucleation process and the growth and coalescence of separate islands have a fundamental importance for the formation of the film structure, i.e. the size of crystallites, their orientation, etc. We shall therefore deal with these stages in more detail.

4.2 Nucleation

The particles which have been evaporated from the evaporation source and have reached the substrate, on which a thin film is to be deposited, generally lose part of their energy on impingement. They are attracted to the surface by forces mostly of dipole or quadrupole character and so they become, at least for a certain time, adsorbed on the surface (adatoms).

The energy loss of a particle which has impinged on the surface and then left it is characterized by the accommodation coefficient α defined as follows.

$$\alpha = \frac{T_c - T_v}{T_c - T_s} \tag{4.1}$$

where T_c is the temperature corresponding to the energy of the incident particle (and determined in the main by the temperature of the evaporation source), T_v is the temperature of the emitted particle and T_s the substrate temperature. The coefficient values are in the range from 0 to 1. The zero value pertains to the case of elastic reflection (without energy loss), the unity value to total accommodation, when the particle loses all its 'excessive' energy and its energy state is then fully determined by the substrate temperature. The theoretical explanation has been elaborated for the simplified case of a particle indicent on a one-dimensional chain of connected particles. It has been found that the sticking coefficient is equal in practice to unity if the energy of the incident particles is less than or equal to about 25 times the desorption energy on the substrate. Since the desorption energy is usually about 1 to 4 eV, the upper limit corresponds to temperatures of the impinging particles in the region of 10^5 K, which far exceed temperatures actually used in normal evaporation. It is therefore highly probable that most particles will be physically adsorbed. (When passing from the linear model to the

spatial one, the probability, though decreased, would still remain high.) The adsorbed particles stay on the surface for a certain time τ_s given as

$$\tau_s = \frac{1}{\nu} \exp \frac{Q_{des}}{kT} \qquad (4.2)$$

where ν is the surface-vibrational frequency of the adatoms, k is the Boltzmann constant, Q_{des} the desorption heat of the particle on the given substrate and T the 'temperature' of the particle which is generally between that of the evaporation source temperature and that of the substrate. The particle which has not been fully accommodated has retained a certain 'excess' energy. Due to this energy and the thermal energy from the substrate, the particle moves over the surface. The movement is called migration or surface-diffusion. During its stay on the surface the particle may be chemically adsorbed (chemisorption). The resulting state is of much higher desorption energy and the particle is then rarely re-evaporated (the time of stay, τ_s, is very long). Besides this, it may happen that the particle will meet another one in the course of its surface-diffusion and form a pair with it which has a much lower re-evaporation probability than a single particle (desorption energy increases by the dissociation energy of the formed pair) and thus the conditions for condensation will be prepared.
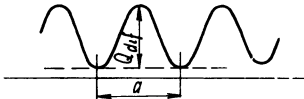

Fig. 40: Potential relief of the surface of a solid.

The condensation coefficient, which gives the ratio of the number of condensed atoms to the total number of impinging atoms, is important in thin film formation. The particle on the surface will move by means of the surface-diffusion to a certain mean distance $\overline{X}$ from the point of incidence. The distance is given as

$$\overline{X} = (2D_d \tau_s)^{1/2} = (2D_d)^{1/2} \nu^{-1/2} \exp\left(\frac{Q_{des}}{2kT}\right) \qquad (4.3)$$

where D_d is the surface-diffusion coefficient. The surface may be represented as in Fig. 40. The binding energy is not the same over the whole surface and the adsorbed particle tends always to occupy the state of minimal energy. Thus it is always localized in some adsorption position (i.e. in some 'valley' of the relief) and to pass into an adjacent position it must overcome a certain

potential barrier — the activation energy for a surface-diffusion jump. The surface-diffusion coefficient is related to this activation energy by

$$D_{\mathrm{d}} = a^2 v \exp\left(-\frac{Q_{\mathrm{dif}}}{kT}\right) \qquad (4.4)$$

Hence we may express the mean distance $\overline{X}$ as

$$\overline{X} = \sqrt{2} \cdot a \exp\left(\frac{Q_{\mathrm{des}} - Q_{\mathrm{dif}}}{2kT}\right) \qquad (4.5)$$

Several values of the magnitude of these quantities are listed in Table 8.

Values for the Desorption Energy Q_{des} *Table 8*
and the Activation Energy for Surface
Diffusion Q_{dif}

	Q_{des} (eV)	Q_{dif} (eV)
Ba on W	3.8	0.65
Cs on W	2.8	0.61
Al on mica	0.9	—
W on W	5.83	1.21
Hg on Hg	—	0.048

If two adjoining nuclei formed by several particles are so near to each other that the regions (roughly of diameter $\overline{X}$) from which other particles can diffuse to them overlap, then the formation of additional nuclei will be practically stopped since all other particles will join existing islands. This implies that the concentration of nucleation centers may be determined from equation (4.5).

To ensure the formation of condensation nuclei, the evaporation rate must be sufficiently high, otherwise a particle migrating over the surface might re-evaporate before meeting another particle. This may be quantitatively expressed as follows. The concentration n_1 of individual particles on the surface is, under the assumption that the impinging flux is $N\!\downarrow$, given by

$$n_1 = N\!\downarrow \tau_{\mathrm{s}}\left[1 - \exp\left(-\frac{t}{\tau_{\mathrm{s}}}\right)\right] \qquad (4.6)$$

The n_1 is constant and equals $N\!\downarrow \cdot \tau_{\mathrm{s}}$ for a sufficiently long duration

of the adsorption $(t \to \infty)$. This means that in a stationary state the impinging current $N\downarrow$ is equal to the flow $N\uparrow$ of re-evaporated particles

$$N\downarrow = \frac{C \cdot p}{\sqrt{(2\pi m k T_v)}} = \frac{n_1}{\tau_s} = n_1 \cdot v \cdot \exp\left(-\frac{Q_{des}}{k \cdot T}\right) \qquad (4.7)$$

where p is the vapor pressure corresponding to the temperature of the evaporation source T_v, C is a constant depending on the geometric configuration of the source and the substrate, and m is the mass of the particle. At very low evaporation rates, the n_1 will thus be very small and the probability of the formation of condensation nuclei will be negligible. The best conditions for their formation and additional film growth will exist at high evaporation rates. During formation and growth of nuclei the process will, of course, not be stationary; the impingement flow is higher than the re-evaporation flow.

The ratio of the impinging flow to the re-evaporation flow $N\downarrow/N\uparrow$ is called supersaturation and it is an important parameter for thin film condensation. The re-evaporation flow is determined by the equilibrium pressure of the evaporant vapor at the temperature of the substrate (e.g. for Ag at 300 °K the pressure is 10^{-40} torr), whereas the impingement flow corresponds to a given evaporation rate (for Ag at 0.1 nm/s evaporation rate, i.e. approximately 1 atom Ag on 1 substrate atom per second, it corresponds to a pressure of $\sim 10^{-6}$ torr).

The conditions under which the condensation begins depend in the main on the ratio of two quantities: the desorption energy characterizing the binding of impinging atoms on the substrate, and sublimation heat, Q_s, characterizing mutual binding of the condensing atoms.

(a) If $Q_{des} \ll Q_s$, the condensation occurs without supersaturation $(P/P_c$ may be less than 1) and the coverage is high.

(b) If $Q_{des} \approx Q_s$, the condensation occurs at a moderate level of supersaturation. This is the region which is satisfactorily explained by the classical theory of nucleation based on thermodynamic concepts (capillarity theory).

(c) If $Q_{des} \gg Q_s$, only very small coverage is achieved under normal conditions and a high supersaturation must be used to effect the condensation. The thermodynamic theory of heterogeneous nucleation is hardly applicable here and it is necessary to use the atomistic theory.

4.2.1 Capillarity Theory of Nucleation

The theory is based on thermodynamic concepts and stems from the Langmuir-Frenkel theory of condensation.

Let us assume that the condensation nucleus has a spherical shape of radius r. During its growth by joining of additional particles (mostly by surface-diffusion) the nucleus energy consisting of the surface and volume components will change. Gibbs's free energy (free enthalpy or Gibbs's potential) ΔG_0 is

$$\Delta G_0 = 4\pi r^2 \sigma_{cv} + \tfrac{4}{3}\pi r^3\,\Delta G_v \qquad (4.8)$$

where σ_{cv} is the condensate-vapor interfacial free energy and ΔG_v is the free-energy difference per unit volume of the phase of molecular volume V, condensed from the supersaturated vapor with the equivalent pressure, p, to the state with the equilibrium pressure p_e, i.e.

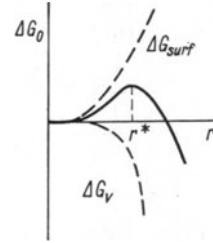$$\Delta G_v = -\frac{kT}{V}\ln\frac{p}{p_e} \qquad (4.9)$$

Fig. 41: The dependence of ΔG_0 on nucleus radius.

Fig. 41 shows the dependence of ΔG_0 on the radius of the nucleus. It can be seen that the r-dependence possesses a maximum at a certain critical radius r^* which can be calculated from the condition

$$\frac{d(\Delta G_0)}{dr} = 0 \qquad (4.10)$$

The r^* value (i.e., radius of the critical nucleus) is therefore

$$r^* = -\frac{2\sigma_{cv}}{\Delta G_v} \doteq \frac{2\sigma_{cv}V}{kT.\ln\dfrac{p}{p_e}} \qquad (4.11)$$

If the radius of the nucleus is smaller than r^*, the nucleus is unstable and there is a high probability that it will disintegrate (the nucleus tends to occupy the lowest energy state which in this case requires disintegration into individual isolated atoms). If the radius is greater than r^*, the energy will decrease with increasing radius so the aggregates will grow until a continuous film is established. We can understand from this how important for film formation is the ratio p/p_e, which is called the supersaturation coefficient.

The nuclei do not have, however, spherical shape, but rather the shape of a spherical cap with a contact angle ϑ determined by the equilibrium of the surface forces (Fig. 42). Denoting the surface free energies by σ, with subscripts s, c, and v referring to the substrate, condensation nucleus and vapor respectively, we obtain

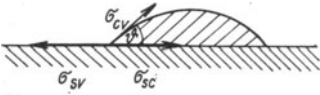$$\sigma_{cv} \cos \vartheta = \sigma_{sv} - \sigma_{sc} \tag{4.12}$$

Fig. 42: The equilibrium of surface forces in nucleus of spherical cap form.

In a manner analogous to that used in equation (4.8), we may also write down Gibbs's free energy in the form of the sum of the surface energy ΔG_1 and the volume energy ΔG_2, which now assume a somewhat more complex structure.

$$\Delta G_1 = \pi r^2 \sin^2 \vartheta (\sigma_{sc} - \sigma_{sv}) + 4\pi r^2 \phi_1(\vartheta) \cdot \sigma_{cv} \tag{4.13}$$

$$\Delta G_2 = \frac{4\pi}{3} r^3 \phi_2(\vartheta) \cdot \Delta G_v \tag{4.14}$$

where $\phi_1(\vartheta)$ and $\phi_2(\vartheta)$ are geometrical factors and ΔG_v has again the form of (4.9). In the refined theory, still another term ΔG_3 is added which represents the entropy of the distribution of the nuclei among n_0 possible positions on the surface of a crystal lattice.

$$\Delta G_3 = - kT \ln \left(\frac{n_0}{n_1} \right) \tag{4.15}$$

The sum of these three terms again reaches a maximum at a certain value r^* and the corresponding critical energy ΔG^* of the nucleus formation; these are given by

$$r^* = - \frac{2\sigma_{cv}}{\Delta G_v} \tag{4.16a}$$

$$\Delta G^* = - kT \ln \frac{n_0}{n_1} + \frac{16\pi}{3} \frac{\sigma_{cv}^3}{\Delta G_v^2} \cdot \phi_3(\vartheta) \tag{4.16b}$$

where ϕ_3 is again a geometric factor given by

$$\phi_3(\vartheta) = \tfrac{1}{4}(2 + \cos \vartheta)(1 - \cos \vartheta)^2 \tag{4.17}$$

Its dependence on ϑ is plotted in Fig. 43.

For complete wetting of the substrate by the condensate when $\vartheta = 0$, only the first term remains in (4.16b); ΔG^* is negative, which makes the situation favorable for the nucleation. In the case of zero wetting, $\vartheta = 180°$, $\phi_3 = 1$ and (4.16b) is transformed into the formula for homogeneous nucleation. This corresponds to the situation when the substrate has no catalytic effect on nucleation.
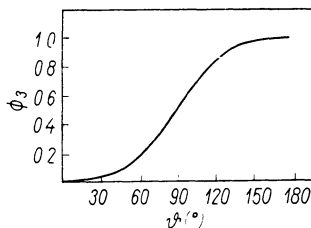

Fig. 43. The dependence of ϕ_3 on ϑ

The quantity ΔG^* may be affected by various factors. For certain values of ϑ, ΔG^* may be, for example, smaller at the steps of a crystal lattice. This is the basis of the surface-decoration effect by means of which it is possible to make the steps visible by coating them with an ultrathin layer of suitable metal which condenses only on these steps (an example of such a decorated surface is shown in Fig. 16). Impurities on the surface may decrease or increase ΔG^*, depending on their nature. Electrostatic charges on the surface reduce ΔG^* and thus facilitate condensation.

The nucleation rate J is very important; it is proportional to the concentration of the critical nuclei N^*,

$$N^* = n_0 \cdot \exp\left(-\frac{\Delta G^*}{kT}\right) \qquad (4.18)$$

where n_0 is the density of adsorption sites, and Γ — the rate at which molecules join the critical nucleus by surface-diffusion. (It follows from a comparison of the relative fractions of the particles joining the nuclei by surface-diffusion and by direct impingement from the vapor phase that the latter mechanism may by neglected.) We have

$$J = Z \cdot 2\pi r^* \Gamma N^* \sin \vartheta \qquad (4.19)$$

Z is Zeldovich's constant and represents the departure of the real state from equilibrium and is about 10^{-2}, $2\pi r^* \sin \vartheta$ is the periphery of the critical nucleus. For the rate Γ we obtain from the diffusion process the relation

$$\Gamma = n_1 \cdot a \cdot v \cdot \exp\left(-\frac{Q_{dif}}{kT}\right) \qquad (4.20)$$

where n_1 is the concentration of adsorbed atoms (see (4.6)). By substitution we obtain the final expression (by using (4.7)):

$$J = Z\, 2\pi r^* n_0 a \sin \vartheta \, \frac{p}{\sqrt{(2\pi mkT)}} \exp\left(\frac{Q_{des} - Q_{dif} - \Delta G^*}{kT}\right) \quad (4.21)$$

(For the meaning of a see Fig. 40). In this expression ΔG_v is incorporated into ΔG^* (see (4.16b)). Thus the nucleation rate is largely dependent on the supersaturation. The quantity ΔG_v has the critical value

$$\Delta G_{vcrit} = -\frac{kT}{V} \ln \left(\frac{p}{p_e}\right)_{crit} \quad (4.22)$$

which corresponds to critical supersaturation. Its significance is obvious from Fig. 44. The dependence of the nucleation rate on supersaturation is very strong: at a supersaturation lower than the critical one J is practically
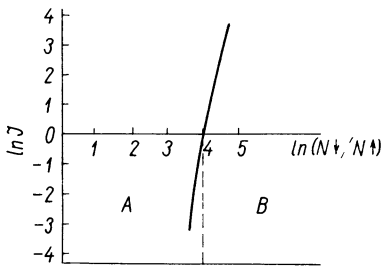

Fig. 44: Nucleation rate as a function of super saturation: A — region where no film formation occurs; B — region of film formation.

zero, whereas at supersaturations higher than the critical one J increases very rapidly $(J \to \infty)$. We speak about the 'onset' of condensation when the nucleation rate reaches about 1 nucleus per second on 1 cm^2.

  If the critical nucleus consists of at least two atoms and the free energy of its formation from vapor is positive, a certain energy barrier exists which prohibits the formation of a continuous film; the island structure appears. If the barrier is high $(\Delta G^*$ is great), the radius of the critical nucleus is large and so a relatively small number of large aggregates is formed. On the other hand, if the barrier is low (small ΔG^*), a great number of small aggregates is formed and the film becomes continuous even at a relatively small thickness. It is therefore clear that factors will substantially affect the final film structure.

  In the case of silver deposited on glass, we obtain $r^* \approx 0.46$ nm and a supersaturation of 10^{34}; for tungsten under similar conditions $r^* \approx \approx 0.13$ nm, the supersaturation is 10^{106}, and the film is very soon continuous.

Supersaturation depends at a given temperature on evaporation heat, which in turn is related to the boiling point T_b by the Trouton relation

$$\Delta L_{vap} = \frac{\Delta H_{vap}}{T_b} \qquad (4.23)$$

where ΔH_{vap} is the enthalpy change. Metals with high boiling point have high values of supersaturation, small-sized critical nuclei and they easily form continuous films. The size of the critical nucleus diminishes considerably whenever there is a strong adhesion between the substrate and evaporated film. The substitution of the theoretical values for the condensation of metal on metal may sometimes result in a negative critical radius. This is not, of course, possible, but it indicates that the critical nucleus contains less than two atoms and that an energy barrier does not exist (no island are formed).

The capillarity theory has enabled us to understand certain basic laws governing thin film formation and has provided a qualitatively correct idea about the influence of particular factors on the initial stage of film growth. Its deficiency rests in that it employs thermodynamic concepts and quantities which apply to macroscopic systems. These concepts may only be employed in cases where the critical nucleus contains more than ~ 100 atoms. In many cases, however, it turns out that the critical nucleus has a radius of several tenths of nm and consists therefore of only a few atoms. In such cases, it is necessary to start with a different theory.

4.2.2 Statistical (Atomistic) Theory of Nucleation

The statistical theory describes the nucleation process when the critical nucleus consists of a very small number of atoms (from 1 to 10). It has been elaborated by Walton and Rhodin [27]. The nuclei are considered as small assemblies, account is taken of the bonds between individual particles and the substrate, and the nucleus is described in terms similar to those used for a macromolecule. These considerations, which we shall not set out in detail here, lead to the following expression for Gibbs's energy of critical nucleus formation

$$\Delta G_i^* = \Delta E_{i0}^* + i^* kT \ln\left(\frac{n_0}{n_1}\right) \qquad (4.24)$$

where E_{i0}^* is the energy of disintegration of the critical nucleus containing i^* atoms at the absolute zero of temperature and n_0/n_1 is the ratio of the number of adsorption sites to the concentration of adatoms.

The expression obtained in this case for the concentration of critical nuclei does not involve macroscopic quantitites such as σ, ϑ, ΔG_v:

$$\frac{n_i^*}{n_0} = \left(\frac{n_1}{n_0}\right)^{i^*} \exp\left(-\frac{E_{i0}^*}{kT}\right) \tag{4.25}$$

and the nucleation rate is given as

$$J = N\downarrow a^2 n_0 \left(\frac{N\downarrow}{\nu n_0}\right)^{i^*} \exp\left[\frac{(i^* + 1)\,Q_{des} - Q_{dif} + E_{i0}^*}{kT}\right] \tag{4.26}$$

The plot of $\ln J$ as a function of $1/T$ can be used for comparison of theory with experiments since it involves measurable quantities. Although the theory does not yield explicit expressions for the calculation of i^* and E_{i0}^*, these quantities may nevertheless be determined by comparing the experimental results with the theoretical ones for different values of i^* and E_{i0}^*. Fig. 45a
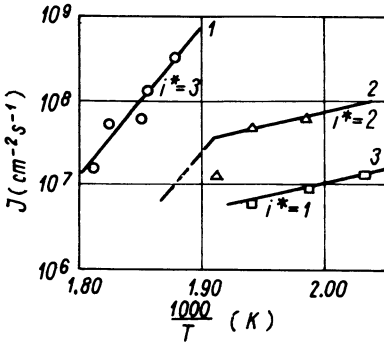

Fig. 45a: Experimentally observed nucleation rate of Ag on (100) plane of NaCl cleaved in vacuum (Rhodin). Deposition rate: (1) $6 . 10^{13}$ cm^{-2} s^{-1}; (2) $2 . 10^{13}$ cm^{-2} s^{-1}; (3) $1 . 10^{13}$ cm^{-2} s^{-1}.
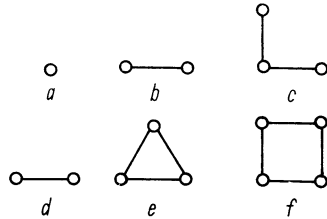
Fig. 45b: Critical nuclei and the smallest stable embryos on the surface of an fcc crystal.

displays results obtained for Ag evaporated onto a single crystal of NaCl in ultra-high vacuum. At very low temperatures of substrate or very high supersaturations, a single atom already represents the critical nucleus. A stable cluster is formed by joining of another atom and the cluster then grows spontaneously. At higher temperatures a pair of atoms with a single bond per atom ceases to be a stable cluster. At this temperature the stable cluster is represented by a group of atoms with at least two bonds per atom (Fig. 45b, where a, b, c are the critical nuclei and d, e, f are the corresponding smallest stable clusters on the surface of a crystal with fcc structure). Since this theory considers the arrangement of individual atoms on the substrate.

surface, it provides information on the structure and orientation of growing clusters.

As the number i^* of atoms in the critical nucleus depends on the temperature of the substrate, there exists a temperature at which a transition occurs from the i^*-atom critical nucleus to the $(i^* + 1)$-atom nucleus.

To give an example: for transition from a 2-atom to a 3-atom stable cluster, the critical temperature is given as

$$T = - \frac{Q_{des} + \frac{1}{2}E_3}{k \ln \left(\frac{N\downarrow}{vn_0}\right)} \tag{4.27}$$

(E_3 is the energy needed for dissociation of a 3-atom nucleus into single particles). The temperature has great significance for the epitaxial growth of films; we shall discuss this in detail later.

The basic equations of the capillarity theory (4.21) and of the statistical theory (4.26) have a similar form, which is understandable since the fundamental principles used in their derivation are identical. The difference lies in the fact that the capillarity theory employs the concept of a continuously varying surface energy and introduces macroscopic thermodynamic quantities, whereas the statistical theory takes into account the discontinuous nature of changes in the binding energy with the addition of a particle to the cluster.

Somewhat different is the statistical theory developed by Zinsmeister (1965—69), which derives from Frenkel's theory of condensation (1924). The basic ideas are approximately as follows: To atoms impinging on a substrate, a certain mean duration and mobility may be assigned. During the staying time there occur collisions which result in the formation of pairs and later in the growth of greater aggregates. The reverse process of aggregate disintegration and re-evaporation proceeds simultaneously.

Let N_i be the concentration of the aggregates containing i atoms, q' the number of atoms impinging on a unit area per unit time, α_i the coefficient characterizing re-evaporation of an i-atom cluster, β_i the coefficient characterizing the disintegration of i-atom aggregates, τ_a the time constant characterizing the re-evaporation, w_{ij} the collision factor pertinent to the collision of i- and j-atom clusters, (is dependent on the coefficient of surface diffusion) σ_i the coefficient characterizing the addition of further particles to the i-atom cluster resulting from direct impingement from the gaseous phase. Then it is possible to set up a system of equations describing the film growth:

$$\frac{dN_1}{dt} = q' + \sum_{i>1} N_i \beta_i - \frac{N_1}{\tau_a} - N_1 q' \sigma_1 - N_1 \sum_{i>1} w_{1i} N_i$$

$$\frac{dN_2}{dt} = \frac{1}{2} w_{11} N_1^2 + N_1 q' \sigma_1 + \sum_{i>2} N_i \beta_i' - w_{12} N_1 N_2 - N_2 q' \sigma_2 - N_2 \alpha_2$$

$$\frac{dN_3}{dt} = w_{12} N_1 N_2 + N_2 q' \sigma_2 + \sum_{i>3} N_i \beta_i'' - w_{13} N_1 N_3 - N_3 q' \sigma_3 - N_3 w_3$$

$$(4.28)$$

The terms containing σ_i are mostly negligible. The w's may be determined from kinetic considerations (for not too high coverage). Since the most prominent role in the dissociation belongs always to the process with smallest dissociation energy, the most significant dissociation will be that of pairs.

The coefficient of pair dissociation may be roughly evaluated as follows: In a solid each atom has 12 neighbors on the average. To effect evaporation, a certain sublimation heat Q_{subl} must be applied. Thus the dissociation of a pair should require $1/6$ of that amount (E_d). Experiments reveal, however, that the real situation is different. The commonly used metals such as Ag, Au, Cu exhibit a much higher pair-dissociation energy $(Ag - 1.6 \, eV, \; Au - 2.23 \, eV, \; Cu - 1.9 \, eV)$. On the other hand, some materials which are known to condense with difficulty (Hg, Cd) have a lower dissociation energy than estimated. This means that in the former case the atom pairs are very stable systems whose dissociation is almost impossible at normal temperatures; the pair is thus a stable cluster. In the case of hard-condensing materials with small E_d the critical nucleus must have $3-10$ atoms. However, E_d may change during the adsorption on the surface of the substrate, especially when the adsorption energy is high.

Thus, if we neglect the dissociation and re-evaporation of pairs and the direct capture of particles from the gaseous phase, it is possible to replace the equation system (4.27b) by a much simpler one:

$$\frac{dN_2}{dt} = \frac{w}{2} N_1^2 - w N_1 N_2$$

$$\frac{dN_3}{dt} = w N_1 N_2 - w N_1 N_3$$

$$\frac{dN_i}{dt} = w N_{i-1} N_1 - w N_1 N_i \qquad (4.29)$$

(All collision parameters are taken equal here, $w_{ij} = w$).

The system may be solved under certain simplifying assumptions. The results are shown in Fig. 46. It is readily seen that bigger aggregates reach their equilibrium concentrations only after the smaller ones. It is also
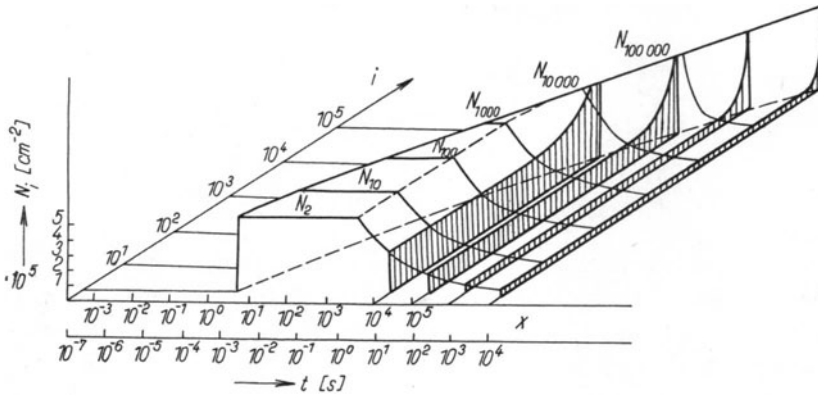
Fig. 46: The time variation of condensation according to Zinsmeister ($q = 10^{13}$, $\alpha = 10^{-7}$, $w = 2 . 10^{-3}$). Concentration of aggregates N_i as a function of real (t) and synthetic (x) time and number of atoms in aggregate.

possible to derive the time variation of the condensation coefficient and the time variation of the amount condensed as a function of the condensation conditions.

While normal condensation is an activated process which starts only when a certain activation energy is supplied for the formation of critical nuclei, the condensation of thin films at high degrees of supersaturation is, according to the aforementioned theory, a simple precipitation which does not need any activation energy. The fact that the condensation sometimes occurs only far below the condensation temperature is due to secondary factors, e.g. evaporation of whole aggregates (which has so far been neglected). The mobility of bigger aggregates is another factor which has been neglected. This mobility decreases with increasing size. Thus the theory should at least take account of the mobility of the twins. The results of calculations can be summed up as follows: The mobility of twins need not be considered if $w_2 < w/1000$. When $w_2 > w/1000$, inclusion of the mobility always leads to narrowing of the size distribution of aggregates and to a decrease in their density G.

The solution of the simplified equation system (4.29) is preceded by introduction of 'synthetic' time by the relation

$$x = w \int_0^t N_1(t)\, \mathrm{d}t \qquad (4.30)$$

$$\frac{\mathrm{d}N_i}{\mathrm{d}t} = \frac{\mathrm{d}N_i}{\mathrm{d}x} \cdot \frac{\mathrm{d}x}{\mathrm{d}t} = N_i' . w . N_1$$

This transforms the system into a set of linear differential equations

$$N_2' + N_2 = \frac{N_1}{2}$$

$$N_3' + N_3 = N_2$$

$$N_i' + N_i = N_{i-1} \tag{4.31}$$

For the comparison with experiments it is important to know the time variation of the size distribution of clusters (i.e. the quantities $N_i(t)$, the numbers of i-atom clusters — or those having diameter D — as functions of time). These quantities may be obtained by solving the differential equations. Fig. 46 shows graphic diagrams of the solutions obtained under certain simplifying assumptions.

The theory predicts dependences of important quantities on basic condensation parameters: the density of aggregates $G = \sum\limits_{2}^{\infty} N_i(t)$ increases with the evaporation rate q $[\text{cm}^{-2} \text{ s}^{-1}]$ as $\sim q^{1/3}$. The maximum cluster diameter D_{max} decreases as $1/q^{1/9}$. Thus an increase in the evaporation rate results in the formation of a higher number of smaller aggregates.

The collision factor w $[\text{cm}^2 \text{ s}^{-1}]$ determining the mobility of adsorbed atoms is related to the aggregate density and maximum cluster size by the relations: $G \sim 1/w^{1/3}$, $D_{\text{max}} \sim w^{1/9}$, i.e. an increase in the surface mobility of particles leads to formation of a smaller number of bigger clusters.

Finally, the temperature of the substrate $T_s[\text{K}]$ influences mainly τ_a which may above all affect the character of the initial stages of condensation. It becomes less important in later condensation stages when it makes itslef felt only through the temperature dependence of the collision factor $w = w(T_s)$.

It is thus seen that the theory yields results which are in qualitative accord with observed dependences. In addition it provides greater possibilities for quantitative comparisons because it gives the time variation of the cluster size distribution. The simplifying assumptions introduced in the original form of the theory have been replaced in subsequent papers by more sophisticated assumptions which better correspond to reality.

4.2.3 Influence of Individual Factors on Nucleation Process

Due to the exponential dependence of J on ΔG^* (or E_i^*), the nucleation rate depends on supersaturation and this in turn depends on the temperature. As we have seen from Fig. 44, J changes very rapidly from negligible values

to very high ones. Critical supersaturation corresponds to a certain critical temperature.

The theories expounded are valid only for 'steady-state' values of J, i.e. when the mean spacing between the nuclei is greater than the diffusion length $\overline{X}$. When the internucleus spacing just equals $\overline{X}$, the density of nuclei reaches a maximum and increases no further. The nuclei grow thereafter only by annexing additional particles by surface-diffusion. This saturation density of nuclei is independent of the impingement rate, provided the impinging atoms are accommodated instantaneously, their momentum is not significant and the impingement flow is smaller then the diffusion flow. Under these conditions, the saturation density is given by

$$N_s = n_0 \exp\left(- \frac{Q_{des} - Q_{dif}}{kT}\right) \tag{4.32}$$

As has been shown, only those particles which remain adsorbed on the surface and condense there can take part in a film formation. Their number relative to the total amount impinging is given by the condensation coefficient. This coefficient decreases with increasing substrate temperature and decreasing binding energy of the adsorbate to the substrate. It depends also on the coverage and so it mostly increases during evaporation and approaches unity at the completion of substrate coverage. Table 9 illustrates

The Condensation Coefficient for Cd on Cu (25 °C)				*Table 9*
Deposit of Cd (nm)	0.08	0.49	0.6	4.24
s	0.037	0.26	0.24	0.60

this fact for the condensation of cadmium on a copper substrate at a temperature of 25 °C. The differences in the condensation coefficient caused by temperature variations and the substrate properties are set out in Table 10.

The coefficients have been generally measured in the initial stages of condensation (i.e. at minimum resolvable film thickness).

The condensation coefficient depends considerably on the presence of adsorbed layers on the surface of a substrate. The coefficient has been found to be practically equal to unity for the condensation of Cd on an atomically clean tungsten surface (at pressures of $\sim 10^{-10}$ torr), whereas at

residual gas pressures of $\sim 10^{-5}$ torr, it is much lower and critical super-saturation increases by several orders. In some cases, however, the adsorption of gases on the surface facilitates condensation (e.g. tin or indium condensation on glass is facilitated by adsorption of oxygen). Thus the influence of adsorbed layers depends on the particular condensate-substrate combination.

The Condensation Coefficients for Some Combinations of Materials

Table 10

Condensate	Substrate	Substrate temperature (°C)	s
Au	glass, Cu, Al	25	0.90 − 0.99
	Cu	350	0.84
	glass	360	0.50
	Al	320	0.72
	Al	345	0.37
Ag	Ag	20	1.0
	Au		0.99
	Pt		0.86
	Ni		0.64
	glass		0.31

If $\alpha < 1$, the accommodation on the surface is insufficient, i.e. a state of thermodynamic equlibrium is not attained. In such cases, unusually high values for critical supersaturation have been observed. This fact suggests that the particles on the surface conserve a part of their energy, i.e. they remain 'hot' relative to the surface temperature so that their effective temperature (corresponding to that energy), rather than the substrate temperature, should be used for calculation of critical supersaturation. We shall return to the influence of the energy of impinging particles when dealing with formation of films by cathode sputtering.

The existence of three-dimensional disconnected islands on the substrate surface established by electron microscopy indicates the existence of a nucleation barrier (see Sect. 4.2.1) and the growth of islands primarily due to surface-diffusion. A two-dimensional monolayer arises only in exceptional cases: (a) if the nucleation barrier is small and the particle energy is high, (b) if nucleation occurs in a narrow vicinity of the impingement site on the substrate (i.e. for low substrate temperature or high-melting-point

evaporation material). When the latter condition is satisfied, a high concentration of nucleation centers arises $(10^{15}\ \text{cm}^{-2})$, so that the film is nearly continuous from the very beginning. The equilibrium density of the centers for metals deposited on insulating substrates is usually 10^{10} to $10^{12}\ \text{cm}^{-2}$, which corresponds to 10 to 100 nm spacing. The sizes of the islands at a given growth stage are distributed around a certain mean value.

The density of nucleation centers may be affected also by certain external agents, e.g. by the presence of electric charge on the film which lowers the nucleation barrier and increases the binding energy, or by using so-called 'pre-nucleation'. The latter consists of the evaporation of an ultrathin layer (thinner than a monolayer) of some metal (usually one with a high melting point) onto a substrate on which a continuous film of another substance is to be deposited. The preliminarily evaporated layer facilitates the birth of nucleation centers because it increases the binding energy and it is possible by choosing a suitable combination of substances to attain a continuous coverage even with a very small thickness.

As we have noted, the nucleation occurs preferentially at the sites where the crystal lattice exhibits some irregularity, e.g. at the steps of the lattice. This is utilized in the technique of decoration.

The occurrence of preferred nucleation sites gives rise to the question of the nature of condensation centers in general. Some authors maintain that the centers are always related to a crystal defect, e.g. to the emerging points of dislocations. On the other hand, it has been established from experiments that the nuclei are randomly and isotropically distributed and that their number is no doubt considerably smaller than that of the adsorption sites but considerably higher than the density of defects on the surface of a typical single-crystal plane (at epitaxial growth). It is therefore more likely that nucleation is a random process and that it results from statistical fluctuations in the supersaturation. Another objection to the hypothesis of defect-initiated nucleation may be seen in the fact that the nucleation density is approximately the same for various substrates so that the defect density should be the same for all of them, which is improbable. Further, the logarithm of the density of nuclei is inversely proportional to the temperature whereas the density of point defects increases with temperature.

From the theoretical considerations mentioned in Sects. 4.2.1 and 4.2.2, we can derive the dependence of nucleation on the substrate temperature. Differentiation of the equations for the radius of the critical nucleus (4.11) with respect to the temperature at a constant rate of impingement and substitution of typical values results in a positive derivative, which means that the size of the critical nucleus increases with increasing

temperature. Consequently, the film preserves its island character until higher values of thickness are reached. During metal-on-metal nucleation, in which there is sometimes no energy barrier at all, the barrier may arise at an elevated temperature (i.e. the film, which has originally grown in the form of a two-dimensional formation, is transformed into a film with three-dimensional island-structure).

By differentiating (4.16b) with respect to T (at a constant impingement flow), we again obtain a positive value. This means that the rate of formation of super-critical nuclei decreases rapidly with the temperature. At a higher temperature, more time is needed for the growth of continuous film.

In a similar manner we may investigate the dependence of nucleation on the impingement flux (or evaporation rate).

The derivative of r^* with respect to N at constant temperature is negative, i.e. the rise in evaporation rate results in the diminution of the size of critical nuclei. The derivative of G^* with respect to N at constant temperature is also negative so that the rate of nuclei formation increases with the evaporation rate. Thus, at higher evaporation rates the continuous film may be formed at a smaller average thickness. The relationship is, however, a logarithmic one so that the evaporation rate must be changed considerably before achieving the desired effect.

As will be obvious from the theory the surface-diffusion coefficient does not affect the size of the critical nuclei but it does affect their rate of formation, which decreases exponentially with increasing activation energy of diffusion. If the energy is too high an island grows only by direct impingement of vapor particles and the aforementioned considerations are, of course, no longer valid.

For the activation energy of metal-on-metal diffusion, the following relation holds in many cases:

$$Q_{dif} \approx 0.25 \, Q_{des} \qquad (4.33)$$

Not much is known about the diffusion on nonmetal substrates. It is clear, however, that the activation energy of surface-diffusion cannot be higher than the activation energy of desorption.

The latter significantly affects both the size and formation rate of critical nuclei. The higher the energy, the smaller is the critical nucleus and the higher is the nucleation rate. The binding energies vary from several tenths of eV for van der Waal's forces to several eV for metal binding. The film-substrate binding is sometimes of a chemical nature (e.g. evaporation of Al onto glass produces an interfacial layer of oxide). This leads to a considerable increase in the binding energy and lowering of the nucleation

barrier. The tendency for the formation of islands decreases and this plays a role in the deposition of Al films on glass.

4.2.4 Some Experiments for Verification
of Nucleation Theories

We have seen earlier the capillary theory predicts the existence of a threshold nucleation frequency and critical adatom (adsorbed atom) concentration.

The equation for the nucleation frequency (4.21) may be rewritten as

$$J = \beta \exp \frac{Q_{des} - Q_{dif}}{kT} \exp \frac{-\Delta G^*}{kT} \cdot \tag{4.21}$$

where ΔG^* is a function of ΔG_v and that in turn is a function of the supersaturation (see (4.16b) and (4.9), (4.22)), and β is a coefficient independent of the temperature.

For experimental verification of this theory two approaches are available: (a) the substrate temperature is kept constant and the supersaturation is varied; then

$$J = \beta' \exp\left(\frac{-\Delta G^*}{kT}\right) \quad \text{i.e. } \ln J \sim \frac{1}{T}$$

or (b) both quantities are varied. Then it is convenient to put (4.21) into logarithmic form and express $(\Delta G_v)^2$ as a function of $kT \ln (\beta/J)$. If the theory is valid, the dependence is linear and is called a Pound-plot. A whole number of nucleation experiments has been evaluated in this way an satisfactory results have been produced. Results for nucleation of Ag on NaCl reproduced in Fig. 45a may serve as an example.

As we have mentioned already in Sect. 4.2.2, it is possible to determine some parameters occurring in the atomistic theory by plotting $\ln J$ vs. $1/T$.

According to theoretical assumptions nucleation begins when the adatom concentration reaches a certain level. The assumption has been verified by Gretz with his experiment with a field emission microscope (see Sect. 4.2.41). He deposited various metals (Zn, Au, Cd, Ni) by means of evaporation on the tungsten tip of the microscope. At a given temperature and impingement flow J_v he recorded a time t needed for the formation of a three-dimensional cluster of evaporated substance as indicated by the appearance of a light spot on a fluorescent screen. He obtained a linear dependence of J_v on $1/t$ (i.e., $J_v t$ = constant, which is just the critical concentration of the adsorbed particles). This confirms the validity of the classical nucleation theory.

Another technique employs a microbalance (see Sect. 3.1.1). In this way, Cinti has measured the condensation coefficient of Ag on quartz as a function of time, substrate temperature and impingement flow. Condensation has been found to be a monotonic function of time and neither the critical supersaturation nor the critical intensity of the impingement flow necessary for the initiation of the nucleation have been observed. The critical radii of nuclei derived from the experiments on the basis of the classical theory are of the order of a few tenths of nm. This suggests that the statistical theory should be applied in this case rather than the capillarity theory.

Recently a mass spectroscopy method has come into use for the investigation of the nucleation process. The surface on which a given flow is impinging is placed so that the particles emitted from it may reach directly the ionization chamber of the ion source of a sensitive mass spectrometer. In the experiments of Hudson, Nguyen Anh and Chakraverty, a monopole mass spectrometer was used. This apparatus has made it possible to detect static partial pressures of $\sim 5 . 10^{-12}$ torr, evaporation rates corresponding to a vapor pressure of $\sim 10^{-8}$ torr and desorption rates of $\sim 10^{13}$ molecules/cm^2 s. The transient process has been observed on a sudden change of impingement flow, namely on the opening or closing of a shutter.

On the opening of a shutter the signal corresponding to the rate of desorption from the surface increases exponentially till reaching equilibrium; after closing it the signal decreases again in a roughly exponential manner. The time constant of the process naturally depends largely on the substrate temperature.

The systems investigated were Cd-on-W and In-on-Si. It has been found in the former case that at elevated substrate temperatures a strongly bound phase arises and a double monolayer may be formed without the occurrence of condensation. At lower temperatures a weakly bound phase appears, which may form even tens of monolayers without condensation. The critical supersaturation needed for initiation of the condensation is determined by exposing the substrate, which is heated to a high temperature, to a molecular beam. The substrate temperature is gradually lowered and the desorption rate is recorded. At a certain temperature, T, a sudden drop occurs in the rate, this corresponds to the transition from the equilibrium desorption to the equilibrium corresponding to the evaporation of the condensed phase. According to the results of Hudson, the critical supersaturation is roughly a linear function of $1/T$ and the logarithm of the coverage at the onset of nucleation is a decreasing linear function of $1/T$.

For the system In on Si, the mean life-times of the adsorbed particles have been measured in a similar manner at various temperatures. At lower temperatures (< 1000 K), the curves of the transient process are not ex-

ponential and the time constants calculated from the decrease and increase starting points of the curves differ from each other: they correspond to the time of equilibrium coverage and that of very small coverage. From these data the dependence of the concentration of adsorbed atoms on $1/T$ has been calculated together with the dependence on surface concentration of mean life-time of In atoms on an Si surface (always at a constant impingement flow). It has been found at the same time that both the condensation and accommodation coefficients are equal to unity. It has been also found that condensation occurs when the pressure equivalent to the impinging flow is lower than that of In vapor at the given temperature (i.e. it occurs at an undersaturation of ~ 0.9).

Some of the results of the experiments are rather surprising and cannot be explained on the basis of existing theories, particularly the high coverage in the Cd-on-W system preceding the nucleation proper and the relatively low supersaturation (about $1.6 - 1.8$ instead of $10^6 - 10^{19}$). Nor is it possible to apply the atomistic theory.

In the In- on Si-system the nucleation occurs even at undersaturation. Here, the surface states on silicon may possibly play some role by representing nucleation centers with a high binding energy.

These experiments thus demonstrate that there are cases of nucleation which lie outside the scope of current theories and which thus may become a stimulus for further theoretical investigations.

4.3 Growth and Coalescence of Islands

For the final structure of a film further stages of growth are important, namely, the growth of individual islands and especially their coalescence.

Growth occurs in the main by surface diffusion of adsorbed atoms (adatoms) and their annexation to the surface of the already existing nuclei. The process is sometimes described in forms of a two-dimensional gas of particles adsorbed on the surface: an island of a radius r may be in equilibrium only with a concentration of adatoms given by the Gibbs-Thomson equation:

$$n_t = n_{eq} \cdot \exp \frac{2\sigma V_m}{kTr} \qquad (4.34)$$

where V_m is the volume of an adatom, n_{eq} the concentration of adatoms corresponding to the equilibrium pressure of the vapor of island material at the temperature T determined by a relation analogous to (4.7),

$$\frac{p_{eq}}{\sqrt{(2\pi m k T)}} = n_{eq} \nu \exp\left(\frac{-Q_{des}}{kT}\right) \tag{4.35}$$

σ is the interfacial energy per unit area.

If the mean concentration of adatoms n is greater than the equilibrium concentration n_t, the island will grow; if it is smaller, the island will disintegrate.

According to Chakraverty, the growth rate of an island is always limited by the slower of the two processes cooperating in the growth, i.e. the surface diffusion and interface transfer.

In the case of the process limited by surface diffusion, the theory proceeds from the solution of Fick's second law on the assumption that the concentration of adatoms varies in the island neighborhood from n' at the island fringe, i.e. at the distance $R = r \sin \vartheta$ from the center of the island, to $\bar{n}$ at the distance $R = l \cdot r \cdot \sin \vartheta$, where l is the screening distance, i.e. the distance at which the concentration again reaches its mean value.

For the growth rate, the relation obtained is

$$J_s = \frac{2\pi D_s}{\ln l} (\bar{n} - n') \tag{4.36}$$

where D_s is the coefficient of surface diffusion.

The rate of interface transfer is determined by the interface area and the difference in the numbers of atoms which join and leave the island. Thus

$$J_t = 4\pi r^2 \, \phi_1(\vartheta) \, \beta_0 (n' - n_t) \tag{4.37}$$

where β_0 is a probability coefficient dependent on the temperature. At equilibrium, both rates must be equal,

$$J_s = J_t = J \tag{4.38}$$

so it is possible to eliminate the unknown quantity n' from (4.36) and (4.37) and thus obtain the following expression for J:

$$J = \frac{(2\pi D_s/\ln l) \, \beta_0 \, 4\pi r^2 \, \phi_1(\vartheta)}{(2\pi D_s/\ln l) + \beta_0 \, 4\pi r^2 \, \phi_1(\vartheta)} (\bar{n} - n_t) \tag{4.39}$$

The time variation of the island volume is

$$\frac{d}{dt}\left[\frac{4}{3}\pi r^3 \, \phi_2(\vartheta)\right] = J V_m \tag{4.40}$$

from which the time variation of the radius is obtained in the form

$$\frac{dr}{dt} = \frac{J V_m}{4\pi r^2 \, \phi_2(\vartheta)} \tag{4.41}$$

$(\phi_1(\vartheta))$ and $\phi_2(\vartheta)$ are geometrical factors which occur in the capillarity theory of nucleation).

Using these concepts. Chakraverty derived an expression for the time distribution of islands at a given time. Similar results may be also obtained by using the statistical theory of Zinsmeister (see Sect. 4.2.2).
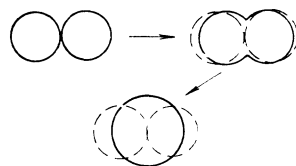

Fig. 47. Schematic illustration of coalescence of two nuclei.

During the following stage of film growth some islands come into mutual contact and coalescence ensues as illustrated in Fig. 47. The islands behave during coalescence like two droplets. By this process the large interfacial energy possessed by the system when comprised of isolated islands is decreased. The nuclei growing on a substrate may have various crystallographic orientations and, in general, various conditions for growth. Large islands grow faster and small ones partly disappear due to the co-alescence with larger ones. At each instant there is a certain size distribution of the islands. It has been found that the distribution is not a Guassian one. It may be observed best by observing film growth directly in the viewing field of an electron microscope, as has been carried out by e.g. Pócza and Barna. An interesting phenomenon is that in some cases the islands assume a crys-tallite shape (with pronounced crystal planes) but behave as a liquid during the coalsecence proper, after which a new crystallite is formed. The pheno-menon of the liquid-crystal and the inverse phase transition may be observed by means of electron diffraction. It is believed that a certain energy is liberated by coalescence which is sufficient to effect a temporary melting of the crystallites in contact. After coalescence the temperature drops and the newborn island again crystallizes. It has been established that when two islands which are of different sizes and crystallographic orientations co-alesce, the resultant crystallite assumes the orientation of the larger one.

This may substantially modify the resulting orientation of the film. It may happen that the nuclei orientations are not evenly represented so that, for example, the [100] orientation prevails over the [111] orientation. If, however, the conditions for growth are better for [111] islands, they will have a greater size when coalescing with those of the [100] orientation. The resulting islands will thus be oriented in the [111] direction so that the [111] orientation may become dominant even when [100] orientation has prevailed during nucleation proper.

Let us return again in more detail to the problem of condensation temperature and to the related problem of the existence of condensate in the liquid or crystalline form. It is necessary to find out whether the condensation occurs by the direct vapor-to-solid transformation or via the vapor-liquid-solid transformation.

Observations obtained by means of electron diffraction seem to indicate that at temperatures higher than $2T_m/3$ (T_m is the melting point of the bulk material) the islands yield diffuse diffraction rings, betraying their liquid nature. This is further sustained by the spherical shapes of the islands observed in the electron microscope. At a temperature lower than $2T_m/3$, the islands yield the diffraction pattern corresponding to a crystalline structure. And, finally, at a temperature lower than $T_m/3$, the diffraction pattern is again diffuse. It would be difficult, however, to assume that a liquid state occurs at such a low temperature. The material should rather be characterized as amorphous.

These observations are explained as follows: The temperature $2T_m/3$ may be very close to the melting point of a small crystallite, which is always lower than that of the bulk material. The melting point T_r of a spherical crystallite of radius r is lowered in consequence of the increase in vapor pressure over the curved surface. According to the Thomson-Frenkel theory the melting point is

$$T_r = T_m \exp\left(\frac{-2\sigma V}{Lr}\right) \tag{4.42}$$

where σ is the liquid-solid interfacial energy, L is the latent heat of fusion and V is the molecular volume of the solid phase. For small differences $T_m - T_r = \Delta T$ one obtains

$$\Delta T = \frac{2\sigma}{r}\frac{T_m}{L} V \tag{4.43}$$

If the radius of the critical nucleus is substituted for r, then

$$\frac{T_m}{T_r} = 1 + \frac{\sigma}{\sigma_{cv}}\frac{kT_m}{L}\ln p/p_r \tag{4.44}$$

Since for many metals $kT_m/L \approx 1$ and $\sigma/\sigma_{vc} \approx 0.1$, it is necessary that $p/p_r \approx 10^2$ if the experimentally found value $T_m/T_r \sim 1.5$ is to be obtained. The value is, of course, many orders lower than the observed levels of supersaturation. Thus the theory does not lead to a quantitative agreement with experiment, but it provides, however, qualitative explanation of the

fact that a substance may condense as a liquid even at a temperature lower than the melting point of the bulk material.

As for the threshold $T_m/3$, the value is not yet substantiated by theory. It is, however, probable that at certain lower temperatures the surface mobility of condensing particles is so low that crystallization cannot occur and the substance assumes the structure of an undercooled liquid.

4.4 Influence of Various Factors on Final Structure of Film

The majority of the physical properties of thin films utilized in practical applications depend to a considerable degree on the structure of the film. It is therefore important to know how particular factors may influence the structure during film growth.

As we have already seen it is not only the nucleation process which is important for the formation of the final film structure but also the process of further film growth. In addition, recrystallization, proceeding especially at elevated temperatures, may also play a role. For the formation of an oriented epitaxial film, it is not sufficient that a large number of nuclei with the given orientation arise at the onset; it is necessary that just these nuclei have optimal conditions for growth so they grow faster than nuclei of other kinds and are of prevailing significance in the recrystallization occurring during coalescence. All these stages may be influenced substantially by impurities on the substrate surface, which explains the great variety of results obtained from the actual observation of the growth of films.

The impurities are bound to the surface with various binding energies. Energies of the order of $0.1-0.5$ eV correspond to physical adsorption, and energies of $1-10$ eV to chemisorption. The influence of impurities depends also on the energy of the impinging particles. The energies for normally evaporated particles are $\lesssim 1$ eV, and for particles in cathode sputtering or those evaporated by special methods (see Sect. 2.3.25) they may be one to two orders higher. We shall be concerned in the next section with the peculiarities of the condensation of a film prepared by these methods.

Surface impurities influence not only the binding energy between the deposited substance and the substrate, and so the size and growth conditions of critical nuclei, but they may even effect a secondary nucleation while no additional nuclei are formed on the clean substrate. Further contamination may lead to the formation of nuclei on the surface of existing islands.

Impurities from the residual gas are also built directly into the film and may influence substantially its resistivity, magnetic properties, etc. At

the same time, it is not so much the total pressure of the residual gas which determines this influence as the partial pressure of some of its components (e.g. oxygen, water).

Further, impurities on the substrate may considerably alter the adhesion of the film to the substrate. The adhesion is strongest when a layer of compound, e.g. oxide, may form in between the film and substrate, as happens, e.g. in the case of iron or aluminium on glass. Adhesion is much weaker if the binding consists of only van der Waals's forces. Even very thin layers of a substance adsorbed on the surface may prevent the formation of the oxide and thus modify substantially the magnitude of van der Waals's forces. Adsorbed layers of organic substances originating from the vacuum seals or the pumping fluid are especially detrimental to adhesion. Heating the substrate before deposition or a raised temperature of the substrate during deposition often improve film adhesion.

We may also note here that if no compound is formed between the film and substrate, good adhesion may be achieved by a transition layer grown by mutual diffusion. This has been demonstrated, for example, on Cd—Fe, a combination which normally shows weak adhesion. If, however, the film is prepared by cathode sputtering, the impinging particles have a higher energy so that the surface is cleared of oxide, precluding mutual diffusion, the deposition centers have higher binding energy and, finally, the particles themselves penetrate the surface to a greater depth. All these factors result in enhanced adhesion.

Besides the cleanness and structure of the surface and the residual gas pressure, the most important factors are the evaporation rate and substrate temperature. We have dealt with their effect on the nucleation process in Sect. 4.2.4. In addition, the evaporation rate considerably influences the content of the impurities in the film itself as follows from equations (2.4) and (2.5).

4.4.1 Special Properties of Films Deposited by Cathode Sputtering

We have mentioned earlier the fact that particles impinging on a surface in cathode sputtering have substantially higher energies than particles produced by evaporation (tens, sometimes even hundreds, of eV). Such particles obviously behave differently on the surface than slower ones. Above all, they usually retain a considerable part of their energy so that they are able to move overt the surface even at temperatures at which evaporated particles would in practice be localized. On the other hand, those particles with the highest energy may create defects at the site of impingement that will there-

fore have a higher binding energy than adjacent areas of the substrate and thus will become sites of preferential nucleation.

Independently of theoretical considerations, it was found earlier that films (e.g. Ag) prepared by cathode sputtering coalesce into continuous film at smaller mean thicknesses than similar films prepared by evaporation.
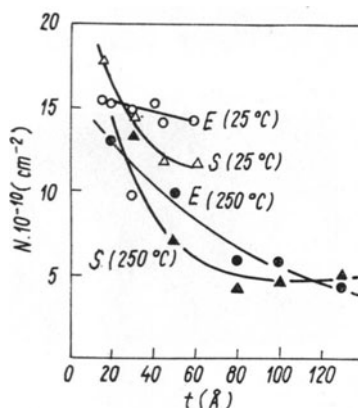

Fig. 48: The variation of the island density N with thickness of Ag film on mica. The films have been prepared by: E — evaporation; S cathode sputtering (Chopra).

Further research, especially that of Chopra, confirmed the results and demonstrated at the same time that it is possible by cathode sputtering to prepare epitaxial films of a high quality similar to those obtainable by evaporation *in vacuo*. Moreover, owing to the greater surface mobility of cathode-sputtered particles, the films have properties similar to those of films evaporated onto the substrate at higher temperatures. The higher nucleation density due to the production of point defects on the substrate surface is enhanced by the influence of the electric charge carried by the particles. The charge also enhances the inter-island diffusion and hence accelerates coalescence. Results of the measurement of island density N vs. film thickness for Ag prepared on mica by the evaporation method (E) and cathode sputtering (S) is illustrated in Fig. 48.

As illustrated, the nucleation density is higher in S at the beginning, which is due to point defects and the influence of the electrostatic charge (the nucleation density is of the same order of magnitude for both S and E, i.e. 10^{11} cm^2). For E at a temperature of 25 °C the density remains practically constant owing to the low mobility, but at 250 °C it decreases. For S the density decreases owing to high mobility even at room temperature and at 250 °C it very soon reaches a constant value, which means that film S is continuous already at a smaller thickness.

Epitaxial growth of evaporated films occur (see Sect. 4.6) only above a certain epitaxial temperature. This depends on both substrate and evapo-
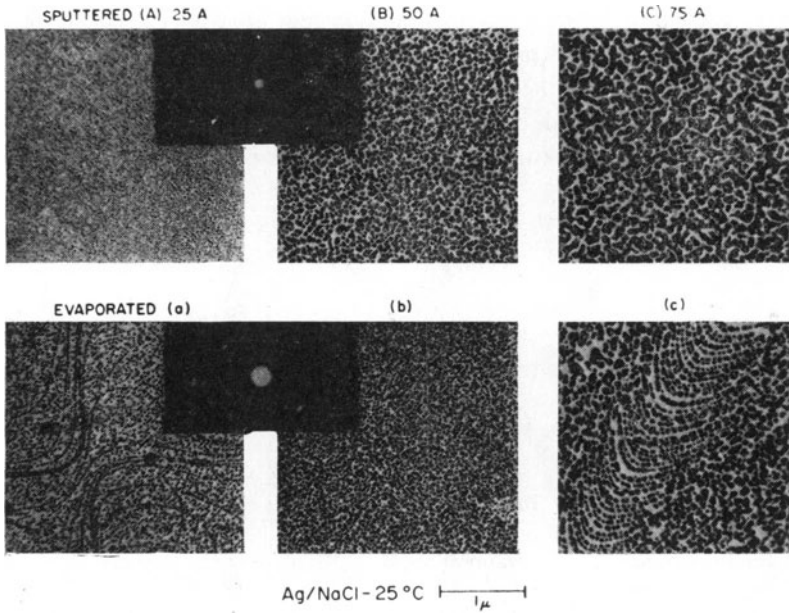
SPUTTERED (A) 25 A   (B) 50 A   (C) 75 A

EVAPORATED (a)   (b)   (c)

Ag/NaCl - 25 °C 1μ

Fig. 49: Films of Ag on NaCl prepared by evaporation and Ar-sputtering at substrate temperature of 25 °C (With permission of Dr. Chopra).
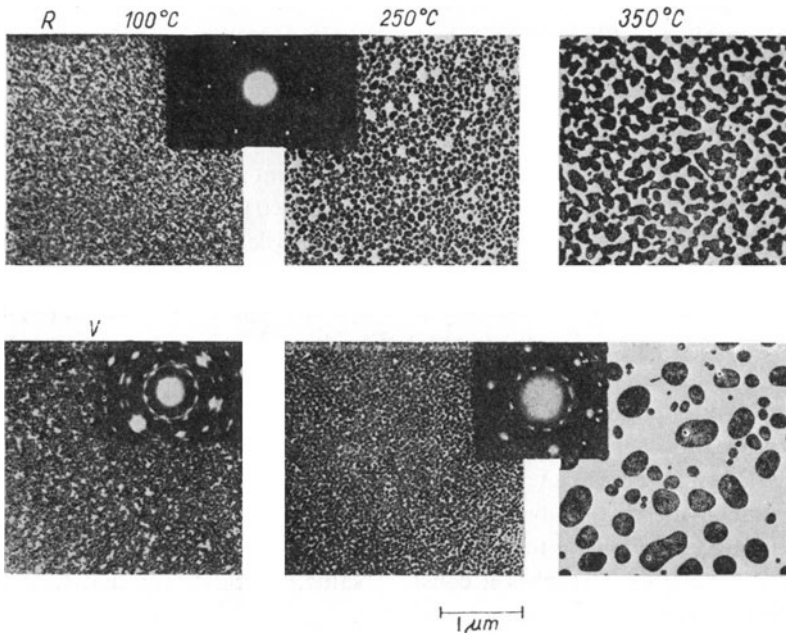

R   100 °C   250 °C   350 °C

V

$1\mu m$

Fig. 50: 10-nm-thick films of Ag: V — evaporated; R — Ar-sputtered on mica at various substrate temperatures (With permission of Dr. Chopra).

rated material and also on the evaporation rate. It has been established that cathode-sputtered films show epitaxial growth at far lower temperatures, sometimes at temperatures below zero. The first row of Fig. 49 shows three electron-microscope illustrations of Ag films deposited by cathode sputtering in Ar onto a single crystal of NaCl at 25 °C; below them are films of the same thickness but prepared by evaporation. In both cases the electron diffractograms are also shown. A certain decorative effect may be observed on the thinnest evaporated film which is not present on the sputtered one owing to higher energies of the particles. Further, there is a difference in the coverage of the thickest films, the sputtered sample showing a greater tendency to uniform coverage of the surface.

In the further illustrations the difference between evaporated and sputtered films can be seen still more clearly. In the first row of Fig. 50 are shown films 10 nm thick, sputtered onto the substrate at various temperatures. Below them are shown analogous illustrations of the evaporated ones. Now, it can readily be seen that at higher temperatures evaporated film forms large droplets on the surface and does not manifest the tendency for growth of continuous film, in constrast to sputtered film. The electron diffractograms (insets) show at the same time that the cathode-sputtered films achieve a perfect monocrystalline structure even at the lowest temperature, whereas in evaporated films partial orientation occurs only after a higher temperature is reached.
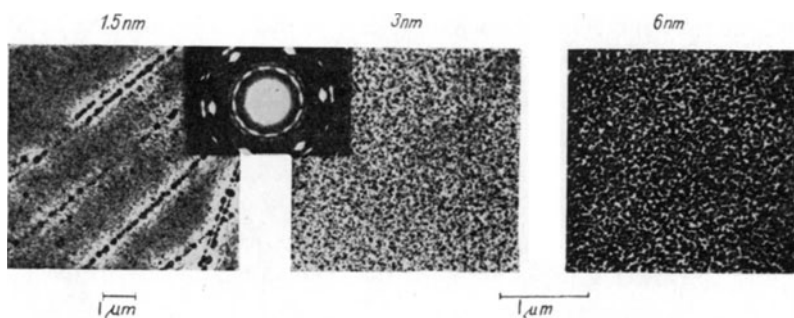

Fig. 51: Ag films of various thickness deposited on mica by He cathode sputtering at 25 °C (With permission of Dr. Chopra).

The question of whether or not these differences in the structure are actually due to the impingement energy of the particles has been solved by sputtering in helium instead of sputtering in argon. Helium has much lighter atoms which carry substantially lower energy to the substrate than argon atoms, provided other conditions are the same. The result of the experiment is shown in Fig. 51. Films have been sputtered at the substrate temperature

of 25 °C, so the conditions are similar to those of the first row of Fig. 49. The electron diffractogram indicates, however, that the film is now only partially oriented, in contrast with that sputtered in argon. This is proof that the energies of the impinging particles play an important role in the determination of film orientation.

Similar results could be expected in films prepared by evaporation by a laser beam or by the exploding-wire method.

4.5 Crystallographic Structure of Thin Films

We have already come across the fact that films may have various crystallographic structures depending on the actual conditions under which they grow. There are essentially three different groups of films: amorphous, polycrystalline and monocrystalline.

Amorphous films are usually formed by such elements as C, Si, Ge, Se, Te, some compounds of Se and Te and by some oxides, if they are prepared with the substrate at room temperature. These are generally the systems characterized by a low surface mobility of adsorbed particles so that the disordered state is frozen before the particles are able to reach the most preferable energetic sites corresponding to the crystallographic structure of the given substance. The amorphous state is therefore a metastable state and such films easily recrystallize with accompanying liberation of energy.

The reduction of the surface mobility of particles which leads to the formation of amorphous films may also be achieved in systems which under normal conditions form crystalline films. The reduction is effected by, for example, admixtures to the residual gas. Oxygen at a pressure of 10^{-4} to 10^{-5} torr prevents the formation of crystallites of easily oxidized substances because the resulting oxide prohibits the coalescence of islands and hence the formation of larger crystallites.

In other films the stabilization of the amorphous state is achieved by different impurities. For example, one atomic percent of nitrogen in the working gas is sufficient in cathode sputtering of W, Mo, Ta and Zr.

There is, in general, an increased tendency for the formation of an amorphous film whenever fast cooling of the condensate is adopted. Pure metals, however, in contrast to elements forming covalent bonds, form crystallites even at liquid helium temperature, though very small ones ~5 nm). The diffraction pattern of such films corresponds to a polycrystalline

structure; it is, of course, a highly disordered state and this fact is shown by the high residual resistance of the film (see Sect. 6.2.1).

The cause of the difference beween metals and substances with covalent bonding is that the small coordination number (the number of nearest neighbors) in covalent-bond materials (4) requires a relatively large displacement of particles if they are to occupy positions which correspond to the crystal structure. Metals, on the contrary, crystallize in close-packed structures in which the arrangement of the particles does not differ as much from the random arrangement. Besides that, they have also lower desorption energy and hence (as adsorbed particles) higher surface mobility.

On metal films it is possible to reduce mobility and obtain an amorphous structure by co-evaporation of two suitably chosen materials, e.g. silver with 16% SiO or tin with 10% Cu. Similar results may be achieved also by cathode sputtering. Such systems usually recrystallize at temperatures of $0.30-0.35$ T_s, where T_s is the mean melting point of both components.

By co-evaporation of two components, it is possible to produce solid solutions of materials which do not dissolve in each other; the solutions thus produced are, of course, metastable. At a temperature of ~ 0.3 T_s the solutions recrystallize and form a single-phase metastable alloy; at a temperature of 0.5 T_s the metastable system disintegrates and a two-phase system is established.

By this means relatively stable systems may be obtained which do not exist otherwise — not only in the form of anomalous alloys and solid solutions but also as pure metals in crystalline forms other than those usually assumed by them. For example, tungsten, molybdenum and tantalum, which crystallize in a cubic, body-centered structure (denoted as bcc) may be prepared in the thin-film form as cubic, face-centered (fcc) materials; the compounds Cds, CdSe, ZnS, ZnSe, etc., which crystallize in the wurtzite structure transform into a sphalerite one, etc. (we shall return to the crystallographic systems later). These anomalous structures are usually rather stable but may be transformed in the normal ones by elevation of the temperature, irradiation with electrons or by treatment with an electric or magnetic field. The transition from the amorphous to the normal crystalline state sometimes proceeds via a succession of metastable states.

Films with a polycrystalline structure may exhibit various crystallite sizes. If the crystallites are smaller than 2 nm, it is not possible (by means of electron diffraction) to distinguish such films from amorphous ones. Indeed, no sharp boundary exists between amorphous and microcrystalline films.

If we are to discuss the crystallographic structure of films in more detail, we should recall some basic concepts of crystallography: We speak

about a crystal when the spatial arrangement of atoms or ions which constitute the substance exhibits certain symmetry and if we can build up the crystal by a periodic spatial repetition of some basic module (primitive cell). According to the symmetry of the cell, determined by three vectors a, b, c of certain lengths which form the angles α, β, γ, we divide the lattices into fundamental crystallographic systems. These are the cubic, hexagonal, trigonal, tetragonal, orthorhombic, monolinic and triclinic systems. In Table 11, the characteristic properties of the basic cells pertinent to the systems are given.

The Parameters of the Primitive Cells in Individual Systems   *Table 11*

System	Characteristic properties of primitive cells
cubic	$a = b = c; \alpha = \beta = \gamma = 90°$
hexagonal	3 coplanar axes at 120° to each other; fourth axis $c \neq a; c \perp a$
trigonal	$a = b = c; \alpha = \beta = \gamma \neq 90°$
tetragonal	$a = b \neq c; \alpha = \beta = \gamma = 90°$
orthorhombic	$a \neq b \neq c; \alpha = \beta = \gamma = 90°$
monoclinic	$a \neq b \neq c; \alpha = \beta = 90° \neq \gamma$
triclinic	$a \neq b \neq c; \alpha \neq \beta \neq \gamma \neq 90°$

It is sometimes convenient to introduce an elementary cell in which the atoms are not confined only to the corners. The symmetry of such a cell corresponds more closely with crystal symmetry and its edges form a simpler coordinate system than the edges of the primitive cell. Fig. 52a shows the elementary cell of the nickel lattice, drawn with a dashed line; the full line is used for the primitive cell. The elementary cell has atoms not only at the
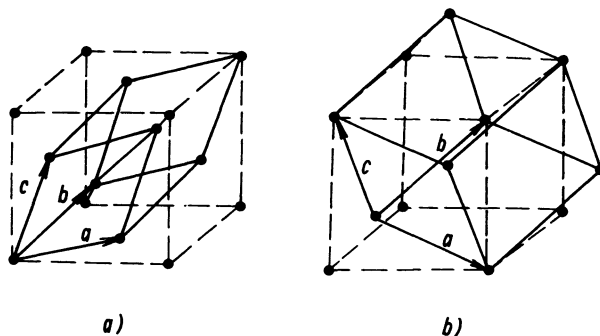

a)   *b)*

Fig. 52: Primitive cell (solid line) and elementary cell (dashed line): (a) face-centered cubic lattice; (b) body-centered cubic lattice.

corners but also in the centres of the cube faces; we speak of the face-centered cubic lattice. In Fig. 52b, both cells of the body-centered cubic lattice are depicted in detail.

Analogously we could construct an elementary cell for the case in which the atoms are in the centers of both bases (base-centered lattice). If we consider the compound cells in all seven crystallographic systems, we obtain fourteen different lattices, called Bravais lattices (their number is not 7 × 4 because some of them are identical). The lattices are illustrated in Fig. 53.
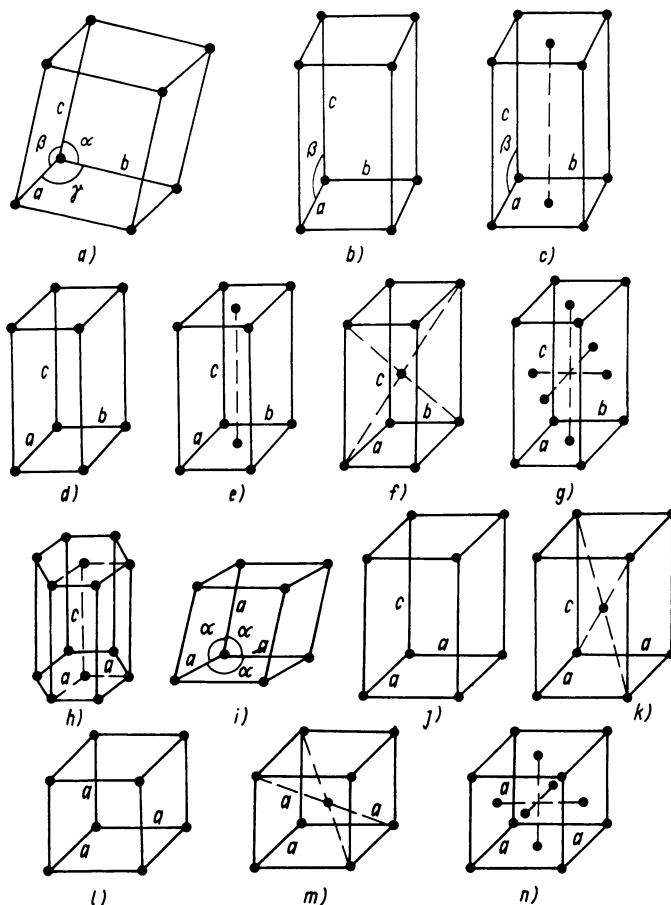

Fig. 53: Bravais lattices: (a) triclinic; (b) simple monoclinic; (c) base-centered monoclinic; (d) simple orthorhombic; (e) base-centered orthorhombic; (f) body-centered orthorhombic; (g) face-centered orthorhombic; (h) hexagonal; (i) rhombic; (j) tetragonal; (k) body-centered tetragonal; (l) simple cubic; (m) body-centered cubic; (n) face-centered cubic.

Crystals are restrained by crystalline planes, which are denoted by the Miller indices introduced for this purpose. Their meaning will first be explained in two-dimensional terms (Fig. 54). Let us pick up a plane which
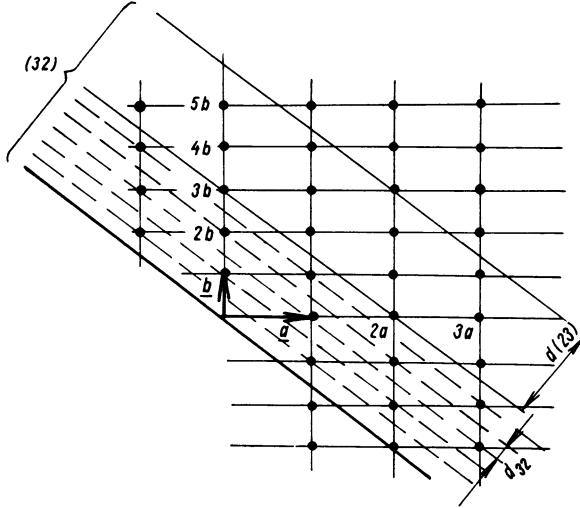

Fig. 54: Illustration for explanation of Miller indices.

passes through the points 2a and 3b (in general P_1a, P_2b). In an analogous manner we could specify a plane in space by intercepts P_1a, P_2b, P_3c, where P_1, P_2, P_3 are relatively prime integers (nonzero) so that the intercepts on the axes represented by them are the smallest integral multiples of the vectors a, b, c for the set of planes parallel to the one selected. The Miller indices are obtained by multiplying the inverse values $1/P_1$ by the smallest common multiple of the P_i.s, i.e. by $P_1\,P_2\,P_3$:

$$(hkl) = \left(\frac{1}{P_1}, \frac{1}{P_2}, \frac{1}{P_3}\right) P_1P_2P_3 = (P_2P_3, P_3P_1, P_1P_2) \qquad (4.45)$$

If, however, the selected plane is parallel to some axis, then the pertinent $P_i = \infty$. The corresponding Miller index equals zero and multiplication by it is omitted. The indices for the example illustrated in Fig. 54 are $(hk) = (32)$.

The indices hkl denote all planes parallel to the basic one which are occupied by atoms arranged in the same manner as in the basic plane. The intercepts cut by these adjacent planes are a/h, b/k, c/l and the perpendicular spacing of the planes is given by

$$d_{hkl} = \frac{d(P_1, P_2, P_3)}{P_1P_2P_3} \qquad (4.46)$$

If the vectors, a, b, c are perpendicular to each other (which occurs in the cubic, trigonal and orthorhombic systems), the realtion may be written as

$$d_{hkl} = \frac{1}{\sqrt{\left[\left(\dfrac{h}{a}\right)^2 + \left(\dfrac{k}{b}\right)^2 + \left(\dfrac{l}{c}\right)^2\right]}} \tag{4.47}$$

In Fig. 55 three significant planes of the cubic system are shown together with their corresponding Miller indices.
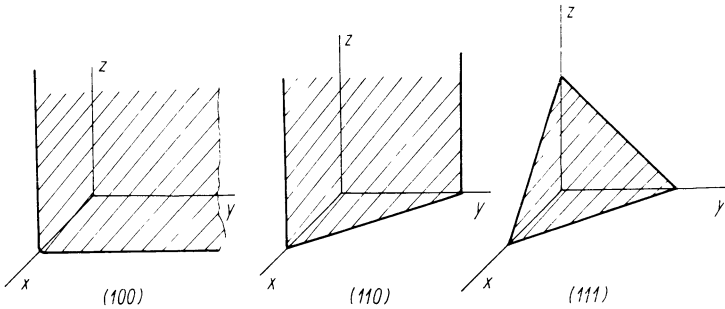

Fig. 55. The most important planes in a cubic system.

If we want to denote a plane intercepting some axis in the negative region, we use a bar placed above the relevant index, as for example, $(0\bar{1}0)$. If the direction of the normal to the plane is to be expressed, Miller indices are placed between brackets, e.g. $[100]$. A set of analogous planes (differing in the sign of the intercepts) is denoted by the indices of the plane with positive intercepts placed in between braces; thus $\{111\}$ denotes the set of planes $(\bar{1}11)$, $(1\bar{1}1)$, $(\bar{1}\bar{1}1)$, $(11\bar{1})$, $(\bar{1}1\bar{1})$, $(1\bar{1}\bar{1})$, $(1\bar{1}\bar{1})$, $(\bar{1}\bar{1}\bar{1})$.
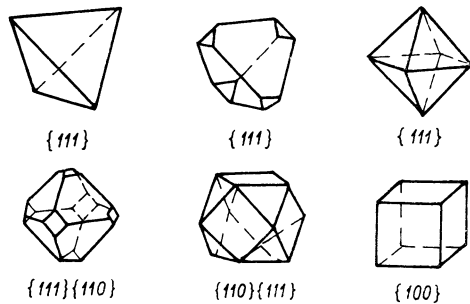

Fig. 56: Some of the most common forms of crystals.

Examples of the shapes of crystals frequently occurring in the domain of thin films, with the respective symbols the planes, are given in Fig. 56. The basic properties of crystals in thin film form are mostly the same as

those of the bulk material. Some special features do, however, exist. If crystallites are very small, a change δd of the lattice constant is observed. The theory gives the following expression for the change:

$$\frac{\delta d}{d} = -\frac{4}{3}\frac{\sigma}{ED} \qquad (4.48)$$

where σ is the surface energy, E is the modulus of elasticity and D the crystallite radius. The expression $4\sigma/D$ denotes the internal pressure in the crystallite, which may be either positive or negative according to the sign and may thus cause an expansion or contraction of the lattice constant. Experimental verification is difficult because it must be carried out on crystals which are entirely stressless and the technique used has to be very accurate. (The moiré method is commonly applied, see Sect. 5.2.) A contraction of the lattice constant with diminishing size of the crystallites has been established in LiF, MgO and Sn.
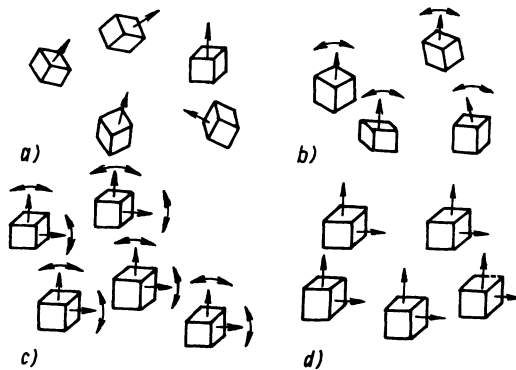

Fig. 57: Orientation of crystallites on substrates (double arrows indicate departures from prevailing orientation): (a) chaotic ordering; (b) single fiber texture; (c) double texture; (d) monocrystalline orientation.

In some cases when the substrate has a lattice constant approaching that of the film (the difference between them being 0.2%), 'pseudomorphism' occurs and the film assumes the structure of the substrate until a thickness of the order of 10 nm is reached. If the difference is greater (4%) and the binding between the substrate and film is strong, then pseudomorphism occurs for only the earliest atomic layers. Still greater differences are accompanied by the formation of lattice defects and dislocations.

Crystals growing on a substrate may be variously orientated. The possible orientations are shown in Fig. 57. Case (a) illustrates a completely disordered film, in which the directions of axes of individual crystallites are

distributed randomly. Case (b) describes a state in which one particular axis of all the crystallites is oriented in approximately the same direction. We speak about a first-stage orientation or a single texture. The common axis is called an axis of texture or a fiber axis. Case (c) depicts so-called second-stage orientation or double texture. Finally, case (d) depicts a mono-crystalline orientation, which is very important because it includes also the case of epitaxial films (see Sect. 4.6).

The single texture, which is also called fiber texture, occurs mainly in metals and semiconductors with homeopolar bond. It may arise during nucleation, after the onset of further crystallite growth or during the complementary tempering.

There are many possible cases of texture growth depending on concrete conditions and certain empirical rules for texture formation have been derived. Phenomenological models proposed hitherto do not, however, take account of all the factors which actually influence texture growth.

Let us present two examples here: Metals with a fcc lattice have, when evaporated onto an amorphous substrate, initially the [111] texture, which transforms into the [110] at greater thickness. The metals crystallizing in the hexagonal system and having a low melting point, together with compounds of the wurtzite structure, assume a well defined [001] orientation in the nucleation stage. For perpendicular incidence the fiber axis is usually close to the normal to the substrate.
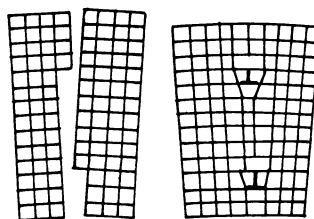

Fig. 58: The origin of dislocations at boundaries of crystallites.

We should mention here defects of crystal lattices in thin films, of which there are a great variety of, e.g. dislocations, point defects, crystal twins, grain boundaries, and stacking faults.

Electron-optical examinations of fcc metals by the moiré technique have revealed that there are almost no defects in separate nuclei and that they arise only after the coalescence process begins. The most frequent defects are dislocations, which arise, for example, at the boundary of two crystal regions that are somewhat angularly displaced with respect to each other (Fig. 58). The density of dislocation lines is about $10^{10} - 10^{11}$ lines/cm^2. These dislocations arise mainly from coalescence of large islands. If the islands are very small, they can move or rotate somewhat to eliminate

the difference in orientation. If they are larger, this is no longer possible and thus dislocations arise in the region of contact. Their number increases especially at the concluding stages of the coalescence of big islands.

Dislocations are also formed on the boundary between film and substrate owing to the difference in their crystal lattices. An overgrowth of substrate defects may also occur in the film. The number of defects in the film is, however, greater by several orders than that of the substrate, so this mechanism is clearly not the main source of the defect. (In single crystals of NaCl, which often serve as substrates for monocrystalline metallic thin films, the defect density is about $10^5/cm^2$.)

The density of some types of defects usually reaches a maximum at 50% coverage; then it decreases with additional deposition and some defects may disappear in continuous films (e.g. twins or stacking faults). The number of defects may be influenced by an additional annealing of the finished film.

The fundamental 'defect' of a crystal lattice is, of course, the surface itself since it represents a cutoff of the periodicity. The surface structure in thermal equilibrium cannot in general conform to that of the bulk material.

The surface particles are arranged in two-dimensional superstructures which may be observed by methods that reveal the structure of only a few atomic layers, e.g. low-energy electron diffraction (see Chapter 5). By this method, the crystallographic symmetry of the surface structure may be determined but it is not yet possible to carry out a complete structural analysis, since the requisite theoretical foundations are still lacking.

A whole number of possible surface arrangements (ordered and disordered structures) exists for a given material, depending on the temperature. At higher temperatures the superstructures of higher orders may appear, i.e. the arrangements with a long-distance periodicity (to hundreds of nm).

4.6 Epitaxial Films

Epitaxy or the oriented growth of films on monocrystalline substrates is a very interesting phenomenon from a theoretical point of view and very important from a practical one.

The term denotes formation of monocrystalline films usually on monocrystalline substrates either of the same substance (e.g. films of Ge on a monocrystal of Ge), when we speak of autoepitaxy (homoepitaxy), or of other substances (e.g. Ag on NaCl), which we term hetero-epitaxy. There are also special cases of growth over an amorphous material or a liquid surface which are called rheotaxy.

The substrate has a very significant influence on the particular orientation of the growing film. Epitaxy can occur between materials of different crystal structure and of different chemical bondings, so the causes of epitaxy are apparently not simple. For example, gold can grow epitaxially on alkali halides, which have a cubic structure, on monoclinic mica and on various crystal faces of single crystals of Ge. The resulting orientation of the film, however, depends in each case on the crystal structure and orientation of the substrate. Thus fcc metals grow on NaCl in parallel orientation with [100], [110], [111] directions, but on mica they grow so that their [111] direction is parallel to the [001] of mica.

Between the planes of substrate and film, which are in mutual contact, some symmetry relations exist (more frequently of rotation than translation symmetry) which may be very complicated.

It was formerly believed that the condition for epitaxy was a degree of correspondence between the lattice constants of the substrate and those of the film. But it has been found that a small difference in the lattice constants ('misfit') is neither a necessary nor a sufficient condition for epitaxy. Epitaxy has been observed even in cases of large misfits of both positive and negative sign.

Studies of epitaxy phenomena deal mostly with the following types: metal on metal, metal on alkali halide or mica, alkali halide on alkali halide, semiconductor on semiconductor.

The fundamental parameter of epitaxial growth is the substrate temperature. For every pair of materials (provided all other conditions are constant), a certain critical epitaxial temperature exists above which epitaxy is perfect and below which it is imperfect. In addition, the epitaxial temperature for a given pair of materials depends on the evaporation rate.

It is obvious from the concepts of thin-film formation set out in this work that an increase in temperature will stimulate epitaxy: desorption of impurities will be facilitated, supersaturation lowered, and surface atoms will have more energy to attain equilibrium sites. At higher temperatures, more of the requisite activation energy (necessary for their mobility) will be supplied to adatoms and thus the recrystallization on coalescence will be facilitated as both surface and bulk diffusion will be enhanced. Higher temperatures may also contribute to the ionization of adatoms. The energy needed for epitaxial growth may also be supplied by other means. It has been observed, for example, that epitaxy may be stimulated by ultrasonic agitation. In Sect. 4.4.1 we have pointed out that the growth of a monocrystalline film is also facilitated by adequately increasing the energy of the impinging particles.

It is difficult to provide precise values of epitaxial temperatures because

the temperature depends on many other parameters. Nevertheless many of these values appear to be reproducible. To give an example, the values of epitaxial temperatures for silver on several different alkali halides are shown in Table 12. It is evident that there is a certain systematic dependence on substrate properties.

Epitaxial Temperature for Ag on Alkali Halides				*Table 12*
	Ag/LiF	Ag/NaCl	Ag/KCl	Ag/KI
T_e (°C)	340	150	130	80

A further significant factor for epitaxy is the deposition rate R. The following equation has been found empirically

$$R \leq A\exp\left(-\, Q_{\text{dif}}/kT_e\right) \qquad (4.49)$$

where A is a constant and Q_{dif} is the activation energy of surface diffusion. This may be expressed in the following way: an adatom must have enough time to jump into a position of equlibrium before it collides with another atom.

A similar relation is derived from the Walton - Rhodin theory of nucleation for transfer from the nuclei with a single bond to those with a double bond (see Sect. 4.2.2).

In some cases epitaxy occurs only at low deposition rates whereas at higher rates crystal twins are formed (i.e. pairs of crystals planes set so that each is a mirror image of the other one). Generally the amorphous, poly-crystalline and monocrystalline phases exist simultaneously in a very wide temperature range.

Another factor influencing epitaxial growth is the contamination which may be caused by an adsorption of residual gas, especially at the higher working pressures. Depending on how the adsorbed substance affects the mobility of adatoms over the substrate, the epitaxial temperature may rise or fall. Some gases (e.g. oxygen and nitrogen) are adsorbed epitaxi-ally on some substrates, and therefore form a surface superstructure which influences further epitaxial growth.

The effect of contamination caused by cleaving of the substrate *in vacuo* ($10^{-4}-10^{-5}$ torr) on the epitaxial temperature is seen from Table 13. The metals concerned here are those growing epitaxially on a (100) surface of NaCl. It is obvious that the epitaxial temperature is lower for the substrate cleaved in vacuum (V) than for analogous films prepared on air-cleaved crystals (A).

Epitaxial Temperature of Films Prepared on Air-Cleaved (A) *Table 13*
and Vacuum-Cleaved (V) (100) NaCl, Respectively

Films	Au	Al	Ni	Cr	Fe	Cu	Ge
$T_e(A)$ (°C)	400	440	370	500	500	300	500
$T_e(V)$ (°C)	200	300	200	300—350	300—350	100	350—400

The question arose whether further lowering of the epitaxial tempera-
ture might be achieved by preparing films on substrates cleaved in ultra-high
vacuum ($\lesssim 10^{-9}$ torr). It has been found, however, that in epitaxial growth
of Cu, Ag and Au on NaCl the epitaxy was inferior (but not for Al and Ni).
Films on crystals cleaved in ultra-high vacuum are sometimes oriented dif-
ferently from the normal, e.g. the (111) orientation appears instead of (100).

This fact suggests that some surface contamination is necessary
for the formation of epitaxial film. It is supposed that in the case of epitaxy
on NaCl, contamination consists in an adsorption of water that etches the
crystal surface and effects a kind of recrystallization favorable for the
growth of epitaxial film.

An additional factor which affects epitaxial growth is the electric
field. It has been observed that growth is accelerated by this field for some
semiconductors (Ge, Si, GaAs) prepared by a chemical trasnport reaction
(see Sect. 2.1).

As we have noted earlier, systems with epitaxial films are very hetero-
genous as to chemical nature and structure, and are also prepared by various
methods, the most important of which are vacuum evaporation, cathode
sputtering and chemical vapor deposition. Because of the complexity of
these phenomena and the presence of so many factors, no consistent and
general theory has as yet been constructed. There are plenty of rules and
hypotheses, most of which deal with special cases and do not cover the whole
phenomena in their totality. Let us set forth here some of the theoretical
ideas.

Brück and Engel [13], for example, assumed for epitaxial growth of
metals on alkali halides that growth proceeds in such a way that the sum
of the distances between the atoms (ions) of the metal and the halogen ions
remains minimal. This corresponds to maximum coulomb forces in the
system. The temperature dependence of epitaxy is explained as a consequence
of the decrease in ionization energy of a metal atom adsorbed on the crystal
surface compared with that of a free atom; this permits ionization to occur
at relatively low temperatures. Epitaxy starts at a temperature at which

the electrostatic interaction with the ionized metal is so strong that the particles can occupy equilibrium positions corresponding to an orientated structure. This theory only described the behavior of systems qualitatively because no quantitative information is known about the decrease in ionization energy. The model is in qualitative agreement with the experimental fact that the epitaxial temperature of metals on alkali halides increases with their ionization energy (e.g. in sequence Ag, Cu, Al and Au).

Another theory assumes that no ionization of atoms occurs on the surface; the atoms are only polarized and thus the effect of temperature operates through a change in atomic polarizability. According to another view epitaxy is realized through two directions with the closest-packed atomic arrangements in the salt being parallel to the two analogous directions in the metal.

Present methods of observation of film structures during their preparation (see Chapter 5) reveal that epitaxy begins to take place in the nucleation stage. Epitaxy should therefore be explained by nucleation theory. However, current theories are not yet developed sufficiently to manage this complex task. For the present they only enable certain relationships to be predicted in a qualitative way.

Thus, according to the capillarity theory of nucleation, it may be expected that for orientations with a lower free interfacial energy on the boundary between the substrate and film, the energy required for the formation of a critical nucleus will be lower so that a higher nucleation rate is to be expected for this orientation.

According to the atomistic model, epitaxy results from the arrangement in the smallest cluster which contains just one more particle than the critical nucleus. If supersaturation decreases, the size of the critical nucleus increases (one, two, three atoms, etc.). A minimum number of bonds exists in a three-atom embryo forming a [111] orientation (for an fcc crystal). The next cluster, of four atoms, forms a [100] orientation, and a five-atom cluster corresponds to a [110] orientation. A similar correspondence has been observed for epitaxial films of Au and Ag. These are, however, very special cases. As yet no general explanation can be advanced to account for even the simplest cases of epitaxy.